Molecular Crystals and Liquid Crystals Science and Technology. Section A. Molecular Crystals and Liquid Crystals
Publication details, including instructions for authors and subscription information:
http://www.tandfonline.com/loi/gmcl19

Patterns in Electroconvection in the Nematic Liquid Crystal 152

Michael Dennin [a], David S. Cannell [a] & Guenter Ahlers [a]
[a] Department of Physics and CNLS, UC Santa Barbara, Santa Barbara, Ca., 93106

Version of record first published: 23 Sep 2006.

To cite this article: Michael Dennin , David S. Cannell & Guenter Ahlers (1995): Patterns in Electroconvection in the Nematic Liquid Crystal 152, Molecular Crystals and Liquid Crystals Science and Technology. Section A. Molecular Crystals and Liquid Crystals, 261:1, 337-348

To link to this article: http://dx.doi.org/10.1080/10587259508033480

Mol. Cryst. Liq. Cryst. 1995, Vol. 261, pp. 337–348
Reprints available directly from the publisher
Photocopying permitted by license only

PATTERNS IN ELECTROCONVECTION IN THE NEMATIC LIQUID CRYSTAL I52

Michael Dennin, David S. Cannell, and Guenter Ahlers
Department of Physics and CNLS, UC Santa Barbara, Santa Barbara, Ca. 93106

Abstract We report on electroconvection patterns in the liquid crystal *4-ethyl-2-fluoro-4'-[2-(trans-4-pentylcyclohexyl)-ethyl]biphenyl* (I52) for two values of the parameter τ_d/τ_σ, where τ_d is the director relaxation time and τ_σ is the charge relaxation time, as a function of the rms voltage and frequency of an applied AC electric field. For $\tau_d/\tau_\sigma = 180$, we observe a forward Hopf bifurcation to a superposition of the two degenerate oblique roll states. The envelopes of these patterns are chaotic in space and time. There exists a secondary transition to a state which oscillates between the two degenerate modes. For $\tau_d/\tau_\sigma = 620$, the initial instability is to a state of stationary oblique rolls. The secondary transition is to a superposition of the already existing oblique rolls and rolls of the same wavenumber which are perpendicular to the existing rolls. This forms stationary oblique squares.

INTRODUCTION

Nematic liquid crystals (NLC) have an inherent orientational order, but no positional order.[1,2] The average direction of their molecular alignment is referred to as the director. By confining the NLC between two glass plates which have been properly treated, one obtains a cell with uniform planar alignment of the director.[3] When an AC voltage is applied across such a cell containing a NLC with a negative anisotropy of the dielectric constant, there is a critical value of the applied voltage, V_c, at which hydrodynamic flows and associated spatially-periodic distortions of the director develop. This is known as electroconvection and is ideal for the study of two-dimensional pattern formation in an anisotropic medium.[4,5] Crucial to the instability mechanism is the presence of a small amount of an ionic impurity.

Unique to anisotropic systems is the existence of oblique-roll states whose wavevectors have nonzero angles with respect to the undistorted director. Because the director is not a vector, states with positive and negative values for this angle are inherently degenerate. For a given wavenumber, we will use the terms zig and zag to distinguish the two degenerate states. The range of existence of oblique rolls is determined by the material parameters.[6,7] As the frequency of the applied voltage

is increased for NLC's which exhibit oblique rolls, the magnitude of the angle of the wavevector decreases continuously from its low frequency value. The frequency at which the angle goes to zero is called the Lifshitz point.[8,9]

An interesting aspect of electroconvection is that detailed stability analyses of the equations of motion have generally led to the prediction of a time-independent pattern immediately above onset,[5,6] whereas experiments have often revealed travelling waves.[10] Various possible theoretical reasons for this conflict have been examined recently.[11] An explanation may possibly be found in a difference between the mobilities of the positive and negative ionic impurities[11,12] which had originally[6] been neglected. This difference is expected to become important when the conductivity σ is relatively small. In the present paper we report new experimental results obtained on samples with carefully measured conductivities, although *systematic* measurements of σ *vs.* drive frequency and voltage for our samples are still under way. We hope that a comparison with detailed theoretical calculations[12] will help to shed light on the origin of the travelling waves seen in the experiments.

The NLC[13] *4-ethyl-2-fluoro-4'-[2-(trans-4-pentylcyclohexyl)-ethyl]biphenyl*, I52, has a strong tendency to form oblique rolls.[7] In this paper, we present studies of the oblique-roll states in I52 for two values of the parameter τ_d/τ_σ, where $\tau_d = \gamma_1 d^2/\pi^2 k_{11}$ is the director relaxation time with γ_1 a rotational viscosity, k_{11} the splay elastic constant, and d the cell thickness, and $\tau_\sigma = \epsilon_o \epsilon_\perp/\sigma_\perp$ is the charge relaxation time where $\epsilon_\perp$ and $\sigma_\perp$ are the dielectric constant and the conductivity perpendicular to the director. For each value of τ_d/τ_σ, we studied the patterns which occurred as a function of the rms amplitude and frequency of the applied voltage. As a test that the ratio τ_d/τ_σ was the relevant parameter,[5] we varied τ_d and τ_σ independently. By changing the thickness of the cell, we varied τ_d, and by changing the conductivity, we varied τ_σ. For $\tau_d/\tau_\sigma = 180$, we observe a superposition of the zig and zag rolls at onset where each set of rolls is traveling. For $\tau_d/\tau_\sigma = 620$, we observe a stationary pattern at onset consisting of separate regions of zig and zag rolls.

In the case of $\tau_d/\tau_\sigma = 180$ we found that the travelling waves are formed *via* a forward bifurcation, and that their amplitudes are chaotic in space and time. Since the bifurcation is forward, one would expect that weakly nonlinear theories should be applicable, and one may hope that the observed spatio-tempora' complexity might be explained on the basis of two coupled Ginzburg-Landau equations, one each for the zig and the zag rolls.

EXPERIMENTAL APPARATUS

The apparatus consisted of a temperature control stage, imaging system, and electronics for applying the AC voltage as well as for measuring the conductivity of the cells. The details of the apparatus are discussed in Ref. 7. The frequency of the applied electric field ranged from 25 to 2000 Hz, and the voltage ranged from 0 to 60 V_{rms}. The temperature control stage maintained the temperature of the cells constant to ± 1 mK.

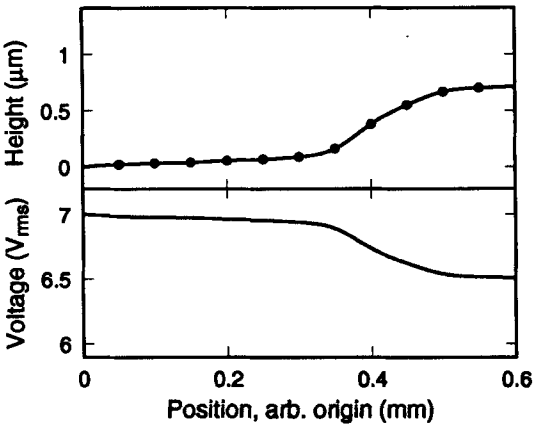

Figure 1 The upper plot shows the thickness of the evaporated SiO layer above the glass plate. The solid circles are taken from a Dektak scan, and the solid line is a spline through the data. The plot shows a region of the cell which extends across one edge of a beach. The bottom plot shows an estimate of the voltage across the cell which was calculated using the curve generated by the spline of the height data. The calculation assumed a dielectric constant of 4 for the SiO layer, a 25 μm thick cell, and a matching SiO layer on the other piece of glass.

The cells used were of two varieties. Cells with a thickness of $d = 10$ μm were obtained commercially.[14] Cells with a larger thickness were assembled by ourselves. We constructed them from 2.5 mm thick glass plates coated with a thin layer of a transparent conductor, indium tin oxide (ITO). The thickness was set by a mylar gasket which was a square of area 2.88 cm^2 with the central 2.25 cm^2 removed. The cells were sealed using Torr Seal. We evaporated a 1 μm thick layer of silicon monoxide (SiO) in 0.2 cm wide strips (beaches) onto the glass slides. The strips formed a square which separated the central 0.25 cm^2 from the outer edges of the

cell. Due to the drop in voltage across the SiO layer, the voltage drop across the I52 is smaller under the beaches than in the central 0.25 cm^2. This ensured that convection occurred first in the central region of the cell, and that it did not propagate in from the mylar spacers. Figure 1 shows a Dektak scan of a typical beach and the resulting profile of the voltage drop across the liquid crystal.

Planar alignment of I52 was obtained using the polyetherimide ULTEM.[15] A polymer film was spin coated onto the glass slides after the evaporation of the beaches. A 1% by weight solution of the polymer in methylene chloride was used. A layer of the solution was placed on the slide and it was spun at 6000 rpm. The resulting film thickness was approximately 1000 Å. The film was then rubbed by hand twelve times using 20 cm long stokes on Extec synthetic velvet.[15]

The I52 was doped using I_2. The initial concentration of I_2 was 2% by weight. Due to rapid evaporation of I_2, the exact concentration at the time the cell was made is not known. Also, once the cells had been sealed, the conductivity, σ, continued to decrease slowly with time. This can be explained by the absorption of I_2 by either the mylar spacers or the epoxy sealing the cell.

The primary method for adjusting τ_d/τ_σ was to vary the conductivity of the cells by changing the working temperature, T. Accounting for the slow drift with time of σ, we found that $\sigma(T)$ increased/decreased in a non-hysteretic fashion as T was increased/decreased. There have been measurements[7,13] of the temperature variation of the anisotropy of the dielectric constant, $\Delta\epsilon = \epsilon_\parallel - \epsilon_\perp$, and γ_1. We have estimated[7] k_{11} at a temperature of 30^o C, but there are no measurements of its temperature dependance. Assuming that the elastic constants and γ_1 have a generic temperature dependance,[2] the ratio γ_1/k_{11} will remain constant to a good approximation in the temperature range studied. Because of the uncertainty in the temperature dependance of the material parameters, we used cells of two different thicknesses at the same temperature. This provided an independent check that τ_d/τ_σ controlled the nature of the observed patterns and not $\Delta\epsilon$ or some other parameter.

EXPERIMENTAL RESULTS

We have detailed observations of the patterns at $\tau_d/\tau_\sigma = 620$ and $\tau_d/\tau_\sigma = 180$ in a cell 25 μm thick made by the procedure outlined in the previous section. In addition to this cell, we report observations of the patterns in a 10 μm high cell. These observations were made to test the relevance of the parameter τ_d/τ_σ.

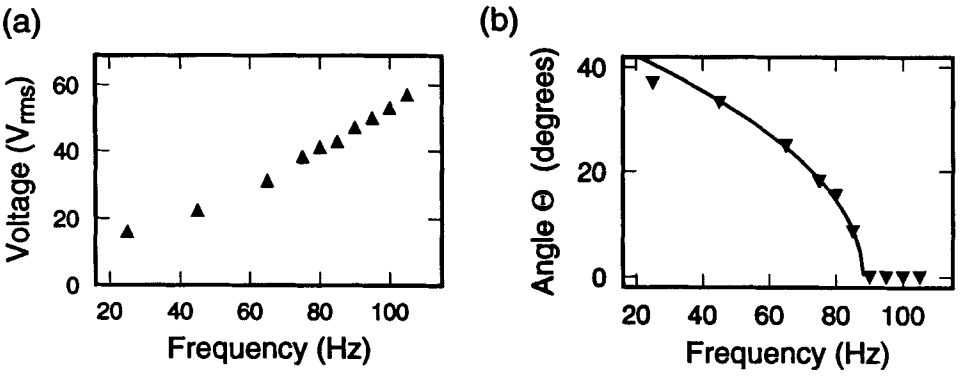

Figure 2 (a) Onset voltage as a function of frequency for $\tau_d/\tau_\sigma = 180$. (b) Angle between the wavevector of the pattern and the director at onset as a function of frequency. The triangles are the measured angle, and the solid line is a fit of $\Theta = a(f_l - f)^{1/2}$ for frequencies in the range of 45 to 85 Hz. We found $f_l = 88.2$ Hz.

For the 25 μm high cell, we studied the case $\tau_d/\tau_\sigma = 180$ at a temperature of 25° C. We measured the onset voltage as a function of frequency by stepping the voltage $\Delta V = 0.004\ V_{rms}$ every 20 minutes. This is shown in fig. 2a. We also determined the Lifshitz point using the square of the spatial Fourier transform of the pattern, $S(k)$, just above onset. A typical $S(k)$ is shown in fig. 3 for a pattern which contains both zig and zag rolls. For a given peak in $S(k)$, we computed the two components of the wavevector,

$$\langle k_x \rangle = \frac{\int k_x S(k)}{\int S(k)} \quad \text{and} \quad \langle k_y \rangle = \frac{\int k_y S(k)}{\int S(k)}.$$

The integrals are computed over a region in k-space which contains only the peak of interest. The angle between the wavevector of the rolls at onset and the director was computed for the zig and zag rolls separately using $\Theta = \arctan(k_y/k_x)$. The two angles were then averaged together. Figure 2b shows this average Θ as a function of frequency. Near the Lifshitz point, Θ should go to zero as a square root law ($\Theta \propto (f_l - f)^{1/2}$). Our results are consistent with such behavior, but more quantitative data are desirable. Previous results[4,16] on the behavior of Θ in electroconvection have not been in such good agreement with the theory. In these cases, it is likely that the bifurcation was backward and that Θ was measured for the finite-amplitude state. As we will show below, for our case there is a forward bifurcation and our measurements were made very close to it. Berge, et al. [17] have reported a detailed

measurement of the behavior of the pattern near the Lifshitz point in Rayleigh-Bérnard convection and found excellent agreement with the expected square root behavior.

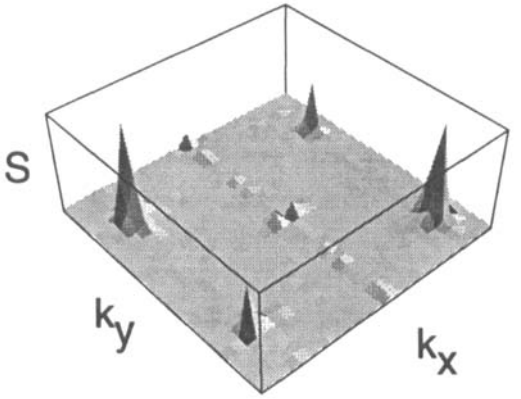

Figure 3 Illustration of $S(k)$ for a pattern containing a superposition of zig and zag rolls. The point $(k_x = 0, k_y = 0)$ is at the center of the plot and the two pairs of main peaks correspond to (k_x, k_y) for the zig and zag rolls. The director is in the k_x direction.

The onset was studied in detail for a frequency of 25 Hz. The pattern at onset is a superposition of the two degenerate oblique rolls at angles of $\pm 37^o$ with respect to the director. As one increases the voltage from below onset, well defined peaks develop in $S(k)$ corresponding to the wavevectors of these two degenerate modes, as was illustrated in fig. 3. The mean squared amplitude of the pattern is taken as the sum of the power under these modes. This eliminates the effect of the peaks in the power spectrum which are a result of known nonlinear optical effects.[18] We used steps of $\Delta V = 0.004\ V_{rms}$, and V_c is defined to be the voltage midway between the value of V for which the mean squared amplitude first became nonzero and the value of V at the previous step. There was a monotonic slow decrease with time of the conductivity which resulted in a corresponding increase of V_c. We made three measurements of V_c over a time period of 140 hours. The measurements were consistent with a linear drift of 1.0 mV/hr. Taking into account this drift in V_c, we computed a value of $\epsilon = (V^2 - V_c^2)/V_c^2$ for each step in the second onset run. The results of this run for the mean-squared amplitude of the pattern as a function of ϵ are shown in fig. 4 and demonstrate that the transition is forward.

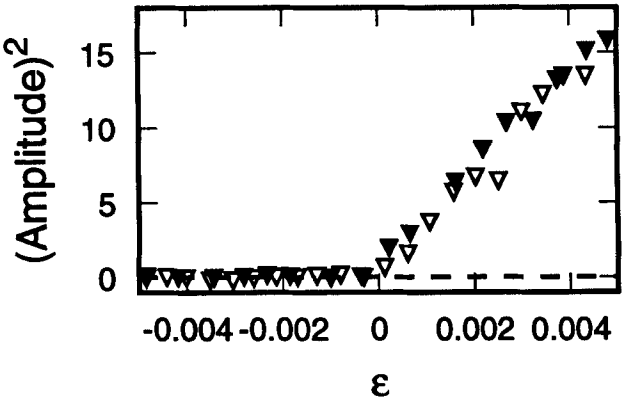

Figure 4 Mean-squared amplitude of the pattern (arbitrary units) as a function of ϵ. The open symbols were obtained by stepping up in ϵ and the closed ones by stepping down in ϵ.

For $f = 25$ Hz, the pattern at onset consisted of traveling waves with an angular frequency of $\omega = 0.2\ s^{-1}$, which corresponds to a dimensionless frequency $\omega\tau_d = 0.11$, and the dynamics suggest the presence of spatio-temporal chaos at onset. Figure 5 shows two images in a time series taken at $\epsilon = 1 \times 10^{-2}$. Also shown is an image of the demodulated zig rolls which clearly shows the defects in the roll structure. The zag rolls have a similar appearance, but with defects in different positions. These defects appear to strongly influence the spatio-temporal dynamics. The forward nature of the bifurcation should make it possible to compare the experiments with predictions based on coupled complex Ginzburg-Landau equations.

There was a secondary transition to a state composed of a superposition of four modes: left and right traveling zig rolls and left and right traveling zag rolls. The boundaries of the region of existence for this state have not been mapped out yet. However, the existence of rolls traveling in both directions is further confirmation that we observed traveling rolls at onset, and not rolls which had a drift due to an inhomogeneity in the cell. Theoretical work with amplitude equations suggests that these patterns are generic to Hopf bifurcations near a Lifshitz point.[19]

The qualitative features discussed above were also observed for $\tau_d/\tau_\sigma = 200$ in a cell at $T = 45^\circ\ C$ which had a thickness of 10 μm. A more detailed study needs to be done to determine if the changes in the material parameters, such as $\Delta\epsilon$, had a

quantitative effect. We also studied the 25 μm thick cell at a temperature of 45° C. This corresponded to $\tau_d/\tau_\sigma = 620$, but small changes in the values for the other material parameters. The observed patterns were very different. The primary and secondary bifurcation curves as a function of frequency and voltage are shown in

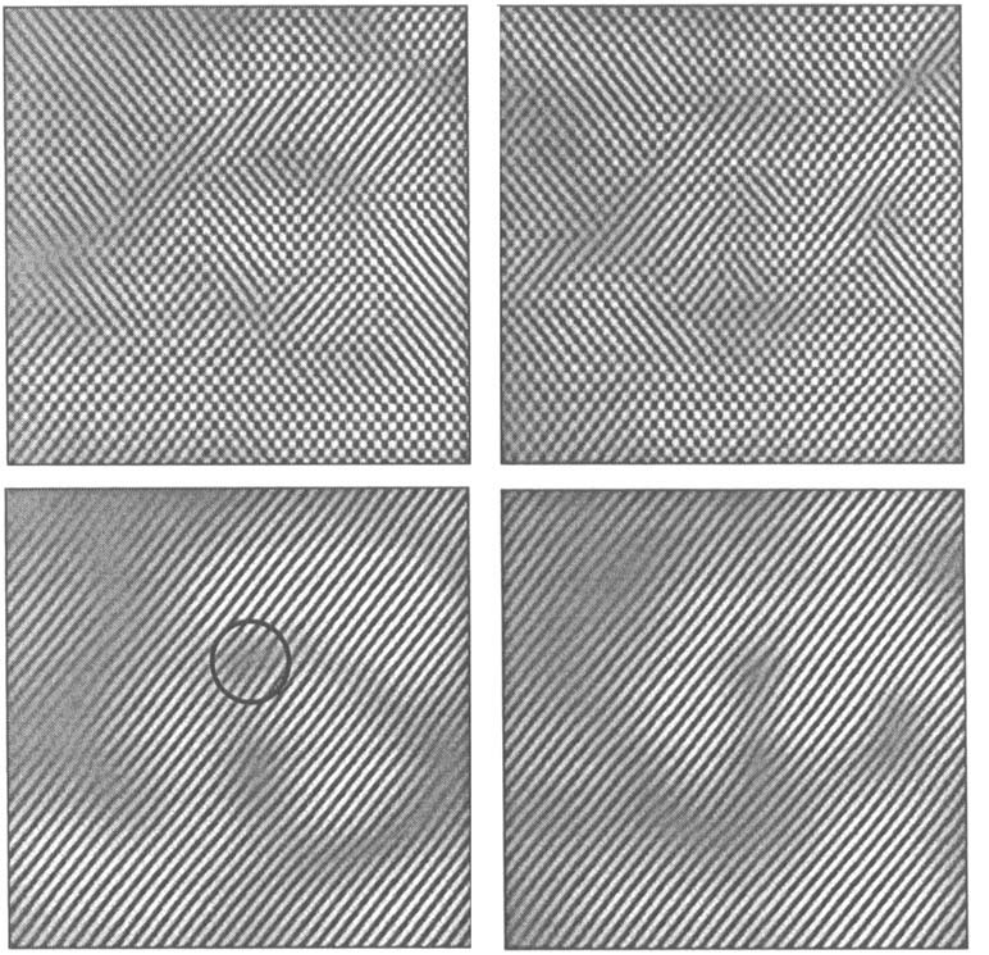

Figure 5 The upper two images are snapshots from a time series at $\epsilon = 1 \times 10^{-2}$ and $f = 25$ Hz (after some digital image processing) separated in time by 1 minute. The lower pair of images are the demodulated zig rolls. The zag rolls have a similar appearance. The mottled nature of the pattern is the result of the amplitude variation with position for either set of the underlying zig or zag rolls. The amplitude variation appears to be controlled by defects with the amplitude going to zero in the neighborhood of a defect. The circled region in the lower lefthand image illustrates a typical defect.

fig. 6. The boundaries were measured using steps of $\Delta\epsilon = 0.01$ every 5 minutes.

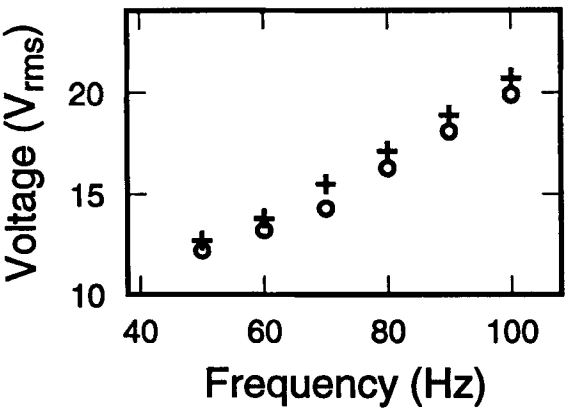

Figure 6 Primary and secondary bifurcation curves for $\tau_d/\tau_\sigma = 620$. The open circles are the primary transition to stationary oblique rolls. The crosses are a secondary transition to oblique squares at $\epsilon \approx 0.1$.

The patterns were stationary at all values of ϵ that were studied. The initial bifurcation was to oblique rolls. At onset, both zig and zag rolls existed in separate regions of the cell. The domains of zig and zag rolls very slowly and continuously changed their size and location through motion of the grain boundaries separating them. This is illustrated in figs. 7a and 7b which show a small section of the cell. In any given region of the cell, the secondary transition was to a state consisting of a superposition of the rolls already present and rolls with a wavevector perpendicular to these. This resulted in squares whose axes were tilted with respect to the director. The direction of the tilt depended on whether the original roll state was a zig or a zag. Preliminary results indicate that there is no change in angle of the original zig or zag rolls at the secondary transition, and the orthogonal set of rolls nucleate in the middle of a zig/zag region, not at the grain boundaries. But, it is not known if the second set of rolls develop continuously or discontinuously. A typical example of one set of the tilted squares is shown in fig. 7c.

We also observed the behavior described above for $\tau_d/\tau_\sigma = 550$ in a 10 μm high cell at a temperature of 65^o C. At this higher temperature, $\Delta\epsilon$ is slightly greater than zero. The small absolute value of $\Delta\epsilon$ at all temperatures does contribute to the existence of the oblique rolls;[6,9] however, this suggests that the sign of $\Delta\epsilon$ is not

critical. The results at this temperature highlight the importance of the assumption that the ratio γ_1/k_{11} is approximately temperature independent. Recalculating τ_d/τ_σ with the assumption that k_{11} is approximately temperature independent, the data is no longer consistent with τ_d/τ_σ being the relevant parameter. One finds that stationary oblique rolls occur at $\tau_d/\tau_\sigma = 125$ in the 10 μm high cell and at $\tau_d/\tau_\sigma = 240$ in the 25 μm high cell. And, instead of occuring at a value of τ_d/τ_σ which is lower than both of these, the superposition of the two degenerate traveling oblique roll states occurs at an intermediate value of $\tau_d/\tau_\sigma = 180$ for the 25 μm high cell. Clearly, measurements of the actual temperature behavior of k_{11} and the other material parameters are necessary to establish conclusively that the relevant parameter is τ_d/τ_σ.

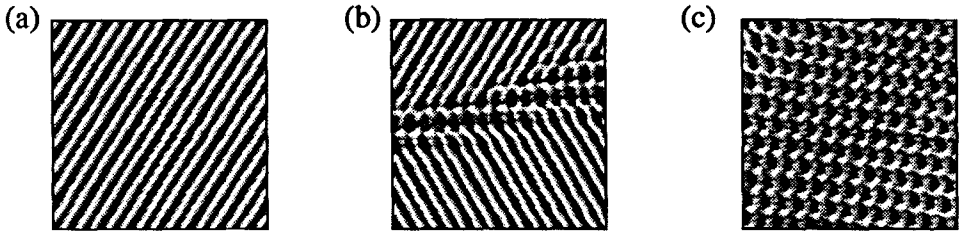

Figure 7 Three typical electroconvection images for $\tau_d/\tau_\sigma = 620$ and $f =$ 65 Hz. Image (a) is at $\epsilon = 0.01$ and corresponds to a small portion of the cell which contains only a single set of oblique rolls. Image (b) is at $\epsilon = 0.07$ and shows a grain boundary between zig and zag rolls. Image (c) is at $\epsilon = 0.11$ and shows a portion of the cell containing only one orientation of the tilted squares.

DISCUSSION

We have observed patterns at two different values of τ_d/τ_σ and discovered very different behavior. For $\tau_d/\tau_\sigma = 180$, we find a forward bifurcation to a state of spatio-temporal chaos. The pattern is a superposition of the degenerate traveling oblique roll states. For $\tau_d/\tau_\sigma = 620$, the pattern consists of coexisting regions which contain only one of the stationary degenerate modes. The overall pattern evolves slowly in time through the motion of grain boundaries between the zig and zag roll states. We also found a secondary transition to a state which is a superposition not of the two degenerate modes but of one of them and a set of rolls orthogonal to it.

The different behavior at the two values of τ_d/τ_σ is reasonable in terms of theoretical considerations.[5,6,11,12] The stability analysis of Ref. 6 predicts a sta-

tionary forward bifurcation to oblique rolls for small values of $\Delta\epsilon$. The analysis is valid for $\tau_d/\tau_\sigma >> 1$. We observe stationary oblique rolls for $\tau_d/\tau_\sigma = 620$. Our observations at $\tau_d/\tau_\sigma = 180$, where we observe traveling rolls, differ from the predictions. Possible reasons may be the relatively small value of τ_d/τ_σ and/or non-ohmic conductivity.[11,12] The variation of the parameter τ_d/τ_σ offers a useful method for testing the range of validity of the theory.

ACKNOWLEDGEMENTS

We wish to thank L. Kramer for very useful suggestions and discussions. This work was supported by the National Science Foundation through grant DMR91-17428. M. Dennin acknowledges support through an Office of Naval Research National Defense Science and Engineering Graduate Fellowship.

REFERENCES

1. L. M. Blinov, *Electro–Optical and Magneto–Optical Properties of Liquid Crystals* (Wiley, New York, 1983).
2. P.G. de Gennes, *The Physics of Liquid Crystals* (Clarendon Press, Oxford, 1973).
3. J. Cognard, *Alignment of Nematic Liquid Crystals and Their Mixtures* (Gordon and Breach, New York, 1982).
4. For a recent review of pattern formation in electro-convection of nematic liquid crystals, see I. Rehberg, B.L. Winkler, M. de la Torre-Juarez, S. Rasenat, and W. Schöpf, *Festkörperprobleme-Advances in Solid State Physics* **29**, 35 (1989).
5. For a recent review of pattern formation in liquid crystals, see L. Kramer and W. Pesch, in *Annu. Rev. Fluid Mech.* **27**, in print.
6. E. Bodenschatz, W. Zimmermann, and L. Kramer, *J. Phys. (France)* **49**, 1875 (1988).
7. M. Dennin, G. Ahlers, and D. S. Cannell, in *Spatio-Temporal Patterns*, edited by P.Palffy-Muhoray and P. Cladis (Addison-Wesley, 1994).
8. R.M. Hornreich, M. Luban, and S. Shtrikman, *Phys. Rev. Lett.* **35**, 1678 (1975).
9. W. Zimmermann and L. Kramer, *Phys. Rev. Lett.* **55**, 402 (1985).
10. See, for instance, Ref. 4, and references therein.
11. W. Zimmermann, in *Nematics: Mathematical and Physical Aspects*, edited by J.-M. Coron, J.M. Ghidaglia, and F. Helein, NATO ASI Series C - Vol. 332 (Kluver Acad. Publishers, Dordrecht, 1991), pp. 401.
12. M. Treiber and L. Kramer, in these Proceedings.

13. U. Finkenzeller, T. Geelhaar, G. Weber, and L. Pohl, *Liquid Crystals* **19**, 123 (1992).

14. Cells and the information concerning their characteristics were obtained from Display Tech Inc., 2200 Central Ave, Boulder, CO 80301.

15. ULTEM is a trademark polyetherimide of General Electric Corporation. Extec was obtained from Excel Technologies.

16. M. de la Torre-Juarez, and I. Rehberg, *Phys. Rev. A* **42**, 2096 (1990).

17. L.I. Berge, G. Ahlers, and D.S. Cannell, *Phys. Rev. E* **48**, 3236 (1993).

18. S. Rasenat, G. Hartung, B. L. Winkler, and I. Rehberg, *Experiments in Fluids* **7**, 412 (1989).

19. M. Silber, H. Riecke, and L. Kramer, *Physica D*, **61**, 260 (1992).